Physical Chemistry Chemical Physics

Supporting Information

Thermochemistry of the Smallest QOOH Radical from the Roaming Fragmentation of Energy Selected Methyl Hydroperoxide Ions

Kyle Covert,[a] Krisztina Voronova,[a] Krisztián Torma,[a] Andras Bodi,[b] Judit Zádor,[c,*] Bálint Sztáray[a,*]

[a]Department of Chemistry, University of the Pacific, Stockton, California, USA

[b]Laboratory of Synchrotron Radiation and Femtochemistry, Paul Scherrer Institute, Villigen, Switzerland

[c]Combustion Research Facility, Sandia National Laboratories, Livermore, California, USA

*Corresponding authors. E-mail: jzador@sandia.gov and bsztaray@pacific.edu.

Contents

SI–1. Cartesian coordinates (Å) and harmonic vibrational frequencies (cm^{-1}) of the structures shown in Fig. 4 of the main text

All structures are determined at the M06-2X/MG3S level of theory, unless otherwise stated.

CH$_3$OOH$^+$

C	-0.002984	-0.008435	-0.053609
O	0.102482	-0.084886	1.399874
O	1.324637	0.091764	1.786308
H	1.295204	0.007491	2.769286
H	0.526084	0.886500	-0.375866
H	0.456133	-0.919204	-0.442254
H	-1.072899	0.026770	-0.227988

29.1951	483.6923	606.2834
828.5928	1113.9179	1148.7260
1330.6078	1422.6025	1452.1987
1462.8266	1509.9920	3062.8506
3168.7436	3226.8508	3568.4040

CH$_3$OOH$^+$ conformer

C	-0.021220	0.016013	-0.031707
O	0.039240	0.097273	1.425486
O	1.206669	-0.008319	1.959336
H	1.895483	-0.132156	1.260508
H	0.572434	0.841997	-0.427463
H	0.359029	-0.966259	-0.317797
H	-1.078306	0.127516	-0.250273

67.1032	473.2391	517.1296
850.3549	1108.6628	1165.1656
1328.0551	1429.9802	1461.9889
1465.9113	1492.1280	3052.4757
3155.8766	3216.2940	3525.1232

[CH$_2$O...H$_2$O]$^+$

C	0.000737	0.003475	-0.000618
O	0.002829	-0.023512	1.202945
O	2.083125	-0.015558	1.656387
H	2.155370	0.747814	2.250859
H	0.937889	0.024461	-0.571840
H	-0.979643	0.006213	-0.503446
H	2.168886	-0.803448	2.216055

212.1816	241.6769	320.5458
373.9409	516.6394	611.5874
1094.1646	1182.9454	1397.3732
1604.2922	1722.0921	2972.7328
3102.3353	3731.8144	3840.9237

[CH$_2$OH...OH]$^+$

C	0.007896	0.000001	0.014667
O	0.016059	-0.000006	1.244733
H	0.939252	-0.000009	-0.554296
H	-0.961698	0.000018	-0.479889
H	0.958546	-0.000022	1.707461
O	2.322841	-0.000044	2.238538
H	2.482606	-0.000050	3.204583

139.4143	159.8340	346.8488
355.9676	507.5663	1209.2487
1231.3247	1264.9931	1502.6054
1518.1836	1753.7538	2413.6618
3099.2929	3236.4984	3691.2243

[HCO...H₃O]⁺

C	-0.000177	0.000131	-0.001229
O	0.003238	-0.009860	1.158789
O	2.536676	-0.002435	-1.026853
H	1.536470	-0.004365	-0.643573
H	-0.889578	0.013498	-0.670528
H	3.020865	-0.827865	-0.850081
H	3.055980	0.771917	-0.747950

55.7697	128.3581	293.6109
390.2926	539.6511	661.8329
1005.8922	1088.4077	1611.6462
1625.5956	2005.9279	2110.2849
2857.5848	3703.5817	3787.2640

[HCO...H₃O]⁺ conformer

C	-0.003154	0.034484	-0.000849
O	0.002289	-0.034955	1.182400
O	1.922205	-0.002717	2.710006
H	1.088690	-0.016013	2.034918
H	2.050314	-0.826223	3.207394
H	1.948812	0.766421	3.301349
H	-0.901826	0.015216	-0.645015

49.0567	141.3610	331.7394
425.6481	526.2876	543.0460
1108.9298	1175.4495	1615.0201
1697.8174	1884.8437	2154.9824
2951.5658	3742.8973	3821.6440

[c-C(H₂)OO(H)⁺]

C	0.166539	-0.040084	0.042389
O	-0.018574	-0.194287	1.401820
O	1.323230	0.122315	0.923230
H	1.481165	1.060584	1.184399
H	0.255783	-0.947812	-0.543807
H	-0.195536	0.881832	-0.400960

780.3845	902.3883	944.0649
1044.8779	1212.2655	1262.5185
1288.0224	1308.7057	1534.9622
3143.3694	3280.0374	3572.7141

CH₃OOH⁺ ↔ [CH₂O...H₂O]⁺ roaming (1e)
(at the MP2/6-311++G level)**

C	0.002083	0.004819	0.000141
O	-0.011037	0.028127	1.270052
O	2.675412	-0.105988	-0.662771
H	3.346751	-0.063133	-1.368749
H	1.173824	-0.040037	-0.309579
H	-0.445275	-0.932505	-0.406327
H	-0.392926	0.949673	-0.440342

-433.8385	50.4221	134.1464
301.9980	434.0817	860.6389
892.3774	1022.0716	1115.1075
1283.2407	1417.1595	1629.1459
2845.9268	2934.7198	3754.1001

CH₃OOH⁺ ↔ [CH₂O...H₂O]⁺ (1f)

C	-0.104079	-0.120885	0.210843
O	-0.256706	0.206209	1.509691
O	1.126042	0.268541	1.872237
H	1.283645	-0.432695	2.546185
H	1.254116	0.129802	0.536437
H	0.276292	-1.136594	0.012487
H	-0.810414	0.340055	-0.469574

-1721.7931	458.9070	578.7971
697.2571	935.8030	987.7497
1058.4422	1138.2958	1213.6007
1347.9788	1466.3955	1682.1145
2980.0700	3236.5863	3589.3142

CH₃OOH⁺ ↔ [CH₂OH...OH]⁺ (1g)

C	-0.075543	-0.116585	0.022172
O	0.127248	0.239005	1.395014
O	1.323585	-0.335629	1.854253
H	1.365428	0.003142	2.769833
H	0.357584	1.069812	0.581160
H	0.672369	-0.780944	-0.389345
H	-1.121686	-0.041848	-0.245762

-1977.3350	302.4360	402.8962
442.3089	878.9118	912.1031
1025.8601	1108.0849	1169.7199
1402.6417	1500.2184	2208.5088
3145.5170	3319.8275	3703.9105

[CH₂O...H₂O]⁺ ↔ [HCO...H₃O]⁺

C	-0.002618	0.000000	-0.000798
O	-0.004391	0.000000	1.183765
O	2.515765	0.000000	0.824904
H	3.060235	0.766402	1.042909
H	1.002435	0.000000	-0.501550
H	-0.962734	0.000000	-0.558865
H	3.060235	-0.766402	1.042909

-199.8563	254.5346	275.1581
282.0735	385.8679	495.8514
853.5180	1129.7321	1231.8549
1647.2786	1720.0318	2707.0121
2930.1572	3800.0308	3896.4606

[CH₂OH...OH]⁺ ↔ [CH₂O...H₂O]⁺

H	0.000000	0.000000	0.000000
O	0.000000	0.000000	1.067009
O	0.369719	0.000000	-1.268284
C	1.577709	0.000000	-1.235027
H	2.109437	0.000000	-0.264169
H	2.130592	0.000000	-2.187152
H	-0.863387	0.000000	1.514584

-1782.4760	108.1775	142.9442
425.1447	580.1565	786.0880
1137.6673	1189.4779	1404.3288
1419.8240	1478.7951	1792.5007
2932.3005	3068.5002	3771.1157

CH$_2$OH$^+$ ↔ HCO$^+$ + H$_2$
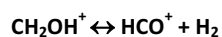
C	0.165423	0.000004	0.138861
O	-0.234284	-0.000520	1.268948
H	1.402932	-0.000575	-0.042195
H	-0.327953	0.000933	-0.844008
H	1.137384	-0.001088	0.951851

-2240.4670	299.1773	1063.4181
1201.0050	1515.5645	1889.4368
2209.0450	2290.4366	3089.1214

CH$_2$OH$^+$ ↔ COH$^+$ + H$_2$
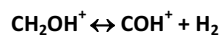
C	-0.000019	-0.000001	0.000021
O	0.000046	0.000004	1.232220
H	1.377411	0.000003	-0.268122
H	0.657566	-0.000003	-0.970297
H	0.812551	0.000010	1.783455

-1795.5659	846.5086	921.5417
1006.8547	1224.5553	1573.5627
1910.4916	2651.0075	3590.1622
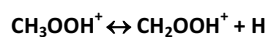
CH$_3$OOH$^+$ ↔ CH$_2$OOH$^+$ + H
(at the M06-2X/6-311++G level)**

C	0.000000	0.000000	0.000000
O	0.000000	0.000000	1.406852
O	1.251533	0.000000	1.735559
H	1.176686	0.000000	2.696669
H	0.492935	0.896090	-0.385925
H	0.856796	-1.557541	-0.670796
H	-1.052839	0.000000	-0.281713

-578.5919	219.4090	305.4380
454.1357	512.3021	820.2564
920.3706	1190.8196	1243.0296
1407.4290	1489.0438	1629.1707
3145.7283	3305.3691	3724.9259

CH$_2$OOH$^+$ ↔ CHO$^+$ + H$_2$O
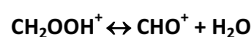
C	-0.022840	0.057019	0.009996
O	-0.093740	-0.247103	1.206045
O	1.406147	-0.311725	1.517132
H	1.604282	0.326295	2.243844
H	1.444220	0.053411	0.371833
H	-1.004546	0.122104	-0.476648

-1922.5596	458.9637	537.8613
871.4707	903.2206	1115.2099
1165.5177	1353.9123	1462.9819
1934.8784	3099.2141	3580.8743

CH$_2$OOH$^+$ ↔ c-C(H$_2$)OO(H)$^+$
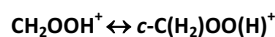
C	0.014906	-0.144520	0.019576
O	0.007390	-0.164128	1.322310
O	1.462027	-0.148722	1.190216
H	1.663819	0.769118	1.470500
H	0.466591	-0.973468	-0.522046
H	-0.526692	0.661752	-0.482098

-770.5986	552.5505	743.5465
948.2548	1208.6793	1246.2819

1340.4478	1434.7269	1561.9108
3085.0306	3237.5425	3660.6481
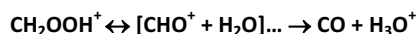
CH$_2$OOH$^+$ ↔ [CHO$^+$ + H$_2$O]... → CO + H$_3$O$^+$
(CCSD(T)-F12 max energy structure along the triplet O-O bond breaking path)

C	-0.422891	0.000001	-1.222652
O	0.566567	-0.000001	-0.539712
O	-0.182901	-0.000001	1.524812
H	0.662122	0.000015	2.032151
H	-1.429944	0.000002	-0.781991
H	-0.282921	0.000001	-2.317412

n.a.

CH$_2$OH$^+$

C	0.000179	0.000152	-0.000025
O	-0.000072	-0.000410	1.239165
H	0.929350	-0.000146	-0.569933
H	-0.978346	0.000954	-0.476040
H	0.874797	-0.001134	1.680872

1025.5485	1113.4142	1266.7308
1381.1429	1496.1364	1714.3991
3113.2403	3253.2288	3646.7628

^{3}CH$_3$O$^+$

C	-0.012538	-0.021716	-0.008866
H	-0.014232	-0.024651	1.116205
H	1.047624	-0.024651	-0.385486
O	-0.622049	-1.077420	-0.439855
H	-0.545160	0.894944	-0.385486

842.0529	842.0600	1141.1774
1141.1781	1238.0495	1248.2855
2725.4872	2751.8354	2751.8367

CH$_2$OOH$^+$
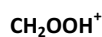
C	0.001315	0.000008	0.000870
O	0.003973	-0.000004	1.236591
O	1.289485	0.000008	1.781805
H	1.094101	-0.000005	2.738657
H	0.943493	0.000027	-0.546940
H	-0.989994	0.000000	-0.446856

306.3033	519.4868	717.7419
939.9378	1199.7799	1248.4000
1428.7326	1499.1051	1721.8556
3112.2957	3260.5715	3713.2040

^{1}CH$_3$OO$^+$

C	0.051653	-0.026935	-0.100503
O	0.305510	-0.331108	1.325267
O	1.050709	0.369783	1.911146
H	0.639237	0.846784	-0.363666
H	0.331773	-0.959374	-0.599508
H	-1.034494	0.100850	-0.130057

192.1249	549.2839	729.3612
1041.5559	1195.4668	1381.2969
1402.9831	1446.4367	1707.0523

3035.0938	3124.8044	3227.5765

$^3CH_3OO^+$

C	0.004669	-0.001274	-0.168740
O	0.168704	0.002627	1.430620
O	1.253305	0.004047	1.932084
H	0.496982	0.921460	-0.459357
H	0.497333	-0.925215	-0.454889
H	-1.076606	-0.001645	-0.237039

	96.0182	328.2417	518.0732
	1062.9573	1096.7323	1396.5173
	1435.1990	1450.8976	1645.9003
	3098.5379	3249.5466	3265.2685

SI–2. Potential energy along the direct dissociation channels of CH_3OOH^+ and details of the related VRC-TST calculations

$CH_3OOH^+ \rightarrow CH_2OOH^+ + H$ (1a)
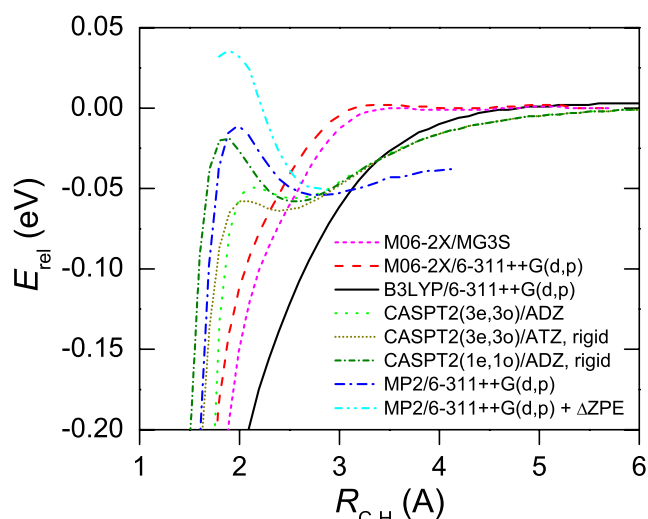
Figure SI–2.1. Energy profiles along the C–H bond in CH_3OOH^+ at various levels of theory. All curves are fully relaxed and ZPE-exclusive, unless noted in the legend. The asymptote is the zero of energy.

This reaction is near barrierless at the M06-2X/MG3S and M06-2X/6-311++G(d,p) levels (there is a slight barrier at ~3.3 Å), while it is barrierless at the B3LYP/6-311++G(d,p) one. With MP2/6-311++G(d,p) we found a barrier at ~2.0 Å, where the barrier is correlated with the planar-to-tetrahedral geometry change along the C–H coordinate. Using CASPT2(3e,3o)/aug-cc-pVDZ we also found this saddle point at ~2.1 Å (the active space consists of the σ and σ* orbitals of the breaking bond and the HOMO). Such variations in the location of this very low barrier are not unexpected and the trends are similar to the findings of Harding *et al.*[1] for neutral species. Using the CASPT2(3e,3o)/aug-cc-pVTZ geometries and ZPE correction we calculated F12 energies for this small barrier and obtained –0.04 eV, and remarkably, the CASPT2(3e,3o)/aug-cc-pVTZ value is also –0.04 eV. These values in case of taking the MP2

geometries are –0.03 and 0.13 eV, respectively. We expect no variational effects to play a role in this region based on the ZPE-corrected potential energy curve for MP2, because the ZPE-corrected maximum coincides with the electronic one along the path, and it is also above the asymptote.

The long-range part of the potential for channel 1a is largely invariant to basis set, active space, and geometry relaxation at the CASPT2 level. Therefore, we sampled the potential at the CASPT2(1e,1o)/aug-cc-pVDZ level between ~3.5 and 15 Å C–H separation of the rigid fragments using overall ~4000 sample points that converged the results to within 5%. At longer distances we only placed the pivot points on the center of mass of the fragments, while at closer separations we calculated fluxes with the pivot point being on the radical carbon atom. In the state counts we also accounted for the OH rotor, but not the C–O one. We found that rotation around the latter bond has a very high barrier and also leads to isomerization at energies higher than the experimental range.
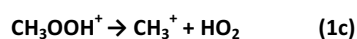
$CH_3OOH^+ \rightarrow {}^3CH_3O^+ + OH$ (1b)
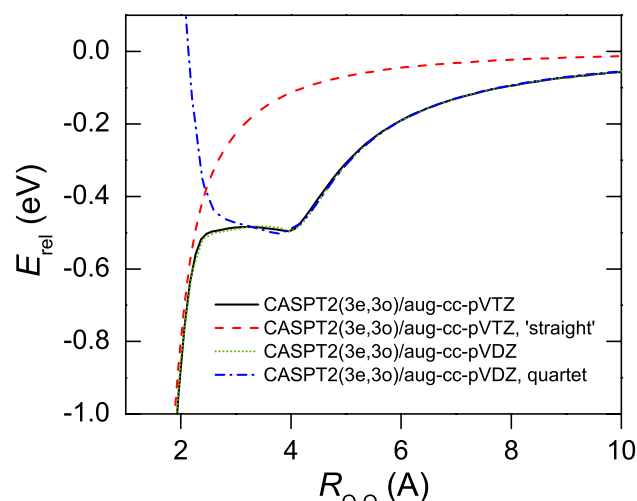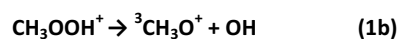
Figure SI–2.2. Energy profiles along the O–O bond in CH_3OOH^+ at various levels of theory. All curves are fully relaxed and ZPE-exclusive. The asymptote is the zero of energy.

To account for the multireference character we calculated the energy along the breaking bond at the CASPT2(3e,3o)/aug-cc-pVTZ level of theory in C_s point group symmetry (A" state) shown in Fig. SI–2.2. The active space consisted of the radical orbital and the bonding and antibonding orbitals of the breaking bond, or, thinking in terms of the fragments, the radical orbital of the OH fragment and the two orbitals occupied by the unpaired electrons of the $^3CH_3O^+$ located on its O atom. The product is $^3CH_3O^+$ because the ZPE-exclusive asymptote at this level is 3.04 eV relative to CH_3OOH^+ and is correlated with the triplet $^3CH_3O^+ + OH$, for which the ZPE-exclusive F12//M06-2X energy is 3.10 eV. $^3CH_3O^+$ is a stable ion and isoelectronic with O_2; the singlet state at the $^3CH_3O^+$ geometry is much higher in energy and readily rearranges to $^1CH_2OH^+$. However, since $^1CH_2OH^+$ is 3.99 eV more stable than $^3CH_3O^+$, it is likely that the latter also eventually forms $^1CH_2OH^+$, but in the mass spectrum

and breakdown curves the two species, if formed this way, are indistinguishable.

Without orbital symmetries we found that it is difficult to converge the doublet state for channel 1b. At the same time the corresponding quartet state, a state that is much easier to converge, becomes degenerate above ~3 Å separation with the doublet one, and the geometry relaxation effects are also negligible in this region. Therefore, we sampled the interfragmental potential at the CASPT2(3e,3o)/aug-cc-pVDZ level of theory for the quartet state between 4 and 20 Å center-of-mass separation to variationally determine the bottleneck for this dissociation channel. We calculated ~6000 points. Due to the spin-orbit coupling of the OH radical we also lowered the asymptote by 70 cm-1 (~0.009 eV) but ignored the rovibronic correction for the OH state count that only affects the lowest ~0.1 eV part of the kinetics.

CH$_3$OOH$^+$ → CH$_3$$^+$ + HO$_2$ (1c)

In addition to M06-2X/MG3S we also scanned this bond using MP2/6-311++G(d,p), and found no barrier either. We also found that above ~3.5 Å, where the potential is already very attractive (−0.4 eV), the fragment geometries are essentially the same as at large separation, demonstrated by the rigid CASPT2(1e,1o)/aug-cc-pVDZ scans, see SI–2.
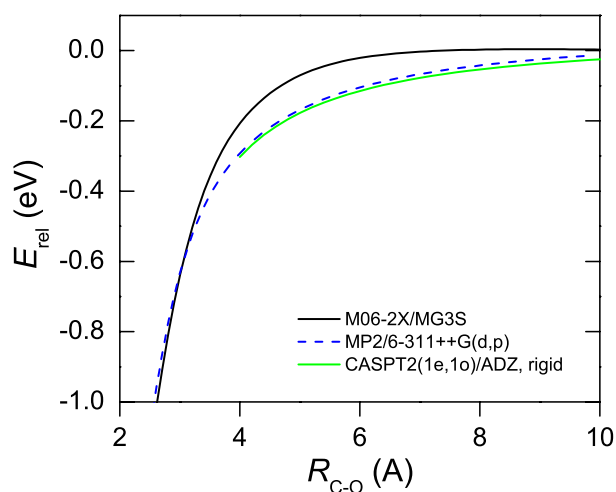
Figure SI–2.3. Energy profiles along the C–O bond in CH$_3$OOH$^+$ at various levels of theory. All curves are fully relaxed and ZPE-exclusive, unless noted in the legend. The asymptote is the zero of energy.

For channel 1c we calculated the number of states using VRC-TST at the CASPT2(1e,1o)/aug-cc-pVDZ level without correcting for geometry relaxation effects. The CASPT2 energies are essentially the same as the MP2 ones in this case. We found that the results are fairly sensitive to the dividing surface optimization in this case, therefore, we sampled interfragmental distances between 2 and 20 Å and placed the pivot points on the center of masses of the two fragments, and at close distances also above and below the plane of

the methyl group at 0.4, 0.8, and 1.0 Å. In total we generated 51 dividing surfaces and ~17000 samples.

CH$_2$OOH$^+$ → CHO$^+$ + H$_2$O   (7c)
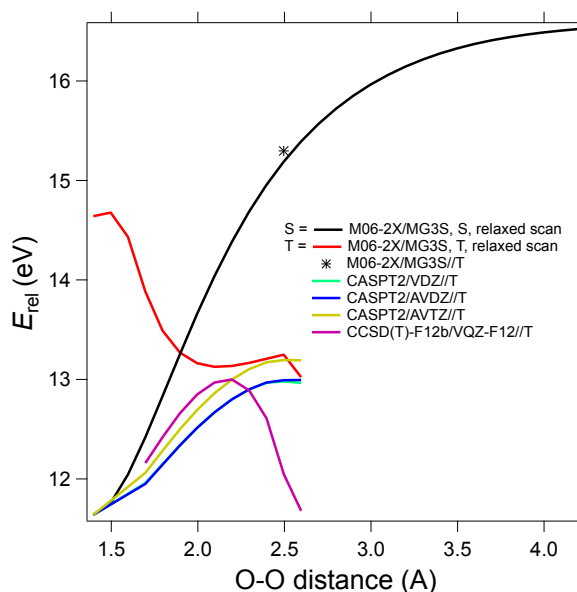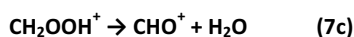
Figure SI–2.4. Energy profiles along the O–O bond in CH$_2$OOH$^+$ at various levels of theory. All curves are ZPE-exclusive, and the energies are shown relative to the neutral CH$_2$OOH. S: geometries along the singlet scan (the OH moiety simply goes away); T: geometries along the triplet scan (the OH moiety stays close to the CH$_2$O part and abstracts an H).

References in SI

1.   L. B. Harding, S. J. Klippenstein, and A. W. Jasper, *Phys. Chem. Chem. Phys.* 2007, **9**, 4055.